Vibrational density of states and homogeneous linewidth in molecular crystals: Many-phonon processes in nitrogen

R. G. Della Valle*
Dipartimento di Chimica Fisica e Inorganica, Università di Bologna, Viale Risorgimento 4, I-40136 Bologna, Italy

G. F. Signorini and P. Procacci
Dipartimento di Chimica, Università di Firenze, Via G. Capponi 9, I-50121 Firenze, Italy
(Received 22 January 1997)

This paper summarizes, simplifies, and extends some recent developments in the theory of phonon damping in anharmonic crystals. We propose an approach in which the damping is described in terms of two ingredients: (1) a computed or estimated one-phonon density of states, and (2) average anharmonic couplings between the phonons, fitted to the experimental temperature dependence of the phonon damping. Solid nitrogen is chosen as a test case and the coupling coefficients obtained from the fit are correlated to the three-, four-, and five-phonon couplings computed from a potential model. [S0163-1829(97)08421-X]

I. INTRODUCTION

The damping of vibrational excitations in pure crystals is due to the anharmonicity of the interaction potential. The lattice vibrations of an ideal harmonic crystal may be described in terms of noninteracting phonons. The anharmonic perturbations lead to interactions in which the phonons exchange energy and are thus directly responsible for the damping. The many-body treatments[1–4] of the phonon interactions indicate that the phonon damping Γ is the sum of an infinite series of contributions (or ''diagrams''), each corresponding to a specific phonon scattering process and with a characteristic temperature dependence.

In principle all kinds of processes involving any number of phonons need to be considered. A physically important and readily interpretable subset of processes is that represented by the ''double vertex'' diagrams.[5] These are n-phonon scattering processes in which a source phonon is annihilated and $n-1$ target phonons are created and/or annihilated, with conservation of the total energy and momentum. It is believed that in many cases, e.g., for weakly anharmonic crystals and for isolated phonon modes, these simple processes are the most probable and give the dominant contribution to the damping.[4–8]

Experimentally the damping Γ is investigated either in the time domain by directly measuring the lifetime Γ^{-1} of the phonon excitations, or in the frequency domain by measuring the phonon linewidth 2Γ. The interpretation of the experiments in terms of decay processes is generally based on the temperature dependence of the linewidth. In this approach a small set of decay pathways is used to fit the experimental temperature dependence.[9] The main limitation of this phenomenological method is the arbitrariness in the choice of the decay pathway. In fact all combinations of phonons with the correct total energy contribute to the damping and there is usually no compelling reason for choosing any particular set of phonon energies. Furthermore, the method does not allow the decay efficiency (i.e., the anharmonic couplings coefficients) to be evaluated separately from the number of available decay pathways.

Recent works[5,10] have demonstrated that very high order contributions to the series for the phonon damping may be computed starting from the crystal potential and that efficient *a priori* calculations of the dampings are feasible. These calculations are based on the separate computation of two ingredients: (1) the number of available decays pathways, i.e., the many-phonon density of states, and (2) the average anharmonic couplings between phonons. The method, which is free of the ambiguities in the phenomenological approach, is, however, dependent on the accuracy of the potential model and is computationally very involved.

This paper proposes an intermediate strategy between the *a priori* computation and the phenomenological fit. In this strategy the many-phonon density of states is computed starting from an experimental or computed one-phonon density, while the coupling coefficients are fitted to the experimental temperature dependence of the phonon linewidth. The coupling coefficients obtained from the fit are defined as averages of potential derivatives and therefore provide information on the crystal anharmonicity. If desired, a direct comparison can be made with the derivatives computed from a potential model. The computational requirements of similar hybrid approaches[11,12] are very moderate, and actually compete with those of the purely phenomenological fit.

Our approach depends on an approximate, but highly efficient, algorithm for computing the damping. Successive terms in the perturbation series for the damping describe scattering processes involving an increasing number n of phonons. The main problem in summing the series for the damping is the explosive growth of the computation time as n increases. This growth is due to (1) the number of processes, i.e., ''diagrams,'' to be taken into account; (2) all the combinations of phonon creation and/or annihilation events for each diagram; and (3) the sum on all branches and wave vectors which must be performed for each phonon involved. If n phonons are involved and the sums are extended to N branches and wave vectors, then the computation time due to (1), (2), and (3) grows approximately as $n!$, 2^n and N^n, respectively, so that the total time grows as $n!2^nN^n$. This ''combinatorial explosion'' is so fast that in practice only the

lowest order contribution to the damping can be computed for realistic models without resorting to drastic approximations.[4,6–8]

The theme of this work and of Refs. 5, 10, and 13 is the need to eliminate all combinatorial factors from the computation time. The growth in the number of diagrams is evaded altogether by considering only the ''double vertex'' diagrams and ignoring all other processes.[5] Only a single diagram is thus considered for each n. This is essentially an uncontrolled approximation, made to allow the calculation to proceed, and justified *a posteriori* by the success of the method.[5] Possible reasons for this success are that the ignored diagrams can be both positive and negative, so that considerable cancellation may occur,[6] and that, by containing several frequency denominators, these diagrams are small in many circumstances.[5] The double vertex diagrams are always positive and contain only a single resonance denominator. These are the diagrams which are usually considered in the phenomenological approach, with the additional constraint of fixed phonon energies; allowing all combinations of energies compatible with the conservation requirements represents at least an improvement with respect to the phenomenological approach.

The complications due to all the 2^n combinations of n creation and annihilation operators are effectively eliminated by a reinterpretation of the meaning of the phonon operators.[5,10] The annihilation of a phonon with energy ω is described as the creation of an ''antiphonon'' with negative energy $-\omega$. In practice this means that all the sums on phonons are extended to both positive (phonon) and negative (antiphonon) energies. All combinations of phonon creation and annihilation processes are thus automatically taken into account. With this method, which involves no approximation, only a single term, rather than 2^n, needs to be taken into account for each n. Obviously, the total number of processes does not change.

This single term has the form of a weighted many-phonon density of states generalized to allow for both positive and negative phonon energies.[5] The direct computation of the n-phonon density by summing over N phonon modes would require a time proportional to N^n. We find[5,13] that, within a reasonable approximation which essentially corresponds to the introduction of an average anharmonic coupling, each of these densities can be recursively computed from the previous density in a time *independent* of n. Therefore the total time for computing the damping due to all double vertex processes involving up to n phonons is *linear* in n.

By avoiding all combinational bottlenecks, this spectacular improvement in the algorithmic efficiency makes the calculation of high order contributions to the phonon damping possible.[5] The original recursive algorithm,[5,13] although quite efficient, still had a slow step, namely the sum on phonon branches and wave vectors that was required at each step of the recursion. By transforming the recursion in a very fast repeated convolution with the one-phonon density of states and then by neglecting the dependence of the n-phonon densities on the wave vector, we have now found a way to eliminate even this remaining slow step.

Besides the n-phonon densities, also the anharmonic coupling coefficients are required for the computation of the damping. In a previous investigation on solid N_2,[5] we evaluated the coupling coefficients directly from their definition as averages of potential derivatives. No adjustment to the observed dampings was involved in the calculations, which may therefore be regarded as an *a priori* determination of the coefficients. In this work we treat the coefficients as adjustable parameters, to be fitted to the experimental temperature dependence of the dampings. Because of the availability of *a priori* coefficients,[5] and of the abundance and quality of the experimental data on the decay processes,[14–18] we have chosen crystalline N_2 as an ideal benchmark for the computational strategy.

The paper is organized as follows. Section II describes the construction of the algorithm for the n-phonon densities and all the approximations involved. This section, which is rather formal, may be skipped by a reader only interested in the algorithm itself. A completely self-contained description of the algorithm is given in Sec. III, where a detailed discussion of the fitting procedure is also presented. The method is applied to the phonons of the N_2 crystal in Sec. IV. The results are presented in Sec. V and discussed in Sec. VI.

II. THEORY

A. Many-phonon densities of states

The developments described in this paper are made possible by a recursive algorithm for computing many-phonon densities with a ''factorized'' weight.[13] The n-phonon density of states $G^n(\omega,\mathbf{k})$ is defined as the number of states available for the decay of an elementary excitation with frequency ω and wave vector $\mathbf{k}$ into a set of n phonons $1,2,\ldots,n$, with conservation of energy and momentum:

$$G^n(\omega,\mathbf{k})=\sum_{\mathbf{k}_1\cdots\mathbf{k}_n} g(\omega_1)\cdots g(\omega_n)\,\delta[\omega-(\omega_1+\cdots+\omega_n)] \times\delta[\mathbf{k}-(\mathbf{k}_1+\cdots+\mathbf{k}_n)], \tag{2.1}$$

where a sum on all phonon branches is implicit in the sums on the wave vectors $\mathbf{k}_i$, ω_i stands for $\omega(\mathbf{k}_i)$, $\delta(x)$ is the Dirac delta, and the weights $g(\omega_i)$ are functions of ω_i (e.g., Bose occupation numbers). In $\delta(\mathbf{k})$ we implicitly allow for the periodicity of the reciprocal lattice.[19] In situations where the momentum is not conserved, as in incoherent neutron scattering experiments, the appropriate density is the reduced density of states

$$G^n(\omega)=\sum_{\mathbf{k}_1\cdots\mathbf{k}_n} g(\omega_1)\cdots g(\omega_n)\,\delta[\omega-(\omega_1+\cdots+\omega_n)]. \tag{2.2}$$

For molecular crystals,[5,13] the n-phonon densities $G^n(\omega,\mathbf{k})$ have been found to become essentially independent of $\mathbf{k}$ as n increases. Therefore $G^n(\omega)$ may be used as a $\mathbf{k}$-independent approximation to $G^n(\omega,\mathbf{k})$ for high n. For CO_2 (Ref. 13) and N_2 (Ref. 5) the approximation appears already usable for the two-phonon density G^2.

Due to the presence of nested sums, the time required to compute the n-phonon densities $G^n(\omega,\mathbf{k})$ and $G^n(\omega)$ through Eqs. (2.1) and (2.2) grows exponentially with n, quickly exceeding any reasonable limit. Fortunately, it is

possible to compute $G^n(\omega)$ in time linear in n by noticing[13] that Eq. (2.2) implies a recurrence relation between G^n and G^{n-1}:

$$G^n(\omega)=\sum_{\mathbf{k}_n} g(\omega_n)\sum_{\mathbf{k}_1\cdots\mathbf{k}_{n-1}} g(\omega_1)\cdots g(\omega_{n-1}) \times\delta[(\omega-\omega_n)-(\omega_1+\cdots+\omega_{n-1})] =\sum_{\mathbf{k}_n} g(\omega_n)G^{n-1}(\omega-\omega_n). \tag{2.3}$$

Here we have changed the order of the sums and recognized that the coefficient of $g(\omega_n)$ is actually $G^{n-1}(\omega-\omega_n)$. With the same method one may easily obtain the analogous recurrence relation for $G^n(\omega,\mathbf{k})$:

$$G^n(\omega,\mathbf{k})=\sum_{\mathbf{k}_n} g(\omega_n)G^{n-1}(\omega-\omega_n,\mathbf{k}-\mathbf{k}_n). \tag{2.4}$$

Equations (2.3) and (2.4) offer an efficient way of computing all G^n up to any desired order. In practice the one-phonon density G^1 is computed first by direct sum through Eq. (2.2) or (2.1), then the densities G^2,G^3,G^4, are computed one after the other through the recurrence relation, Eq. (2.3) or (2.4). Each additional density in the sequence requires a constant increment of computer time, so that the total time required up to order n is linear in n. Please note that this result only holds with a factorized weight function $g(\omega_1)\cdots g(\omega_n)$. We are convinced that the computing time for densities with nonfactorizable weights is intrinsically exponential in n. The problem is not solvable in a time which grows as a power of n (i.e., it is NP hard[20]).

Besides their usefulness in the practical computation of G^n, Eqs. (2.3) and (2.4) also indicate that all the information in G^n is already contained in the one-phonon density G^1. In fact, by inserting a δ integral closure, i.e., $G^{n-1}(\omega-\omega_n)=\int d\Omega G^{n-1}(\omega-\Omega)\delta(\Omega-\omega_n)$, in the right-hand side of Eq. (2.3) and then exchanging integral and sum, we can represent G^n as the convolution of G^{n-1} and G^1:

$$G^n(\omega)=\sum_{\mathbf{k}_n} g(\omega_n)G^{n-1}(\omega-\omega_n) =\sum_{\mathbf{k}_n} g(\omega_n)\int d\Omega\ G^{n-1}(\omega-\Omega)\delta(\Omega-\omega_n) =\int d\Omega\ G^{n-1}(\omega-\Omega)\sum_{\mathbf{k}_n} g(\omega_n)\delta(\Omega-\omega_n) =\int d\Omega\ G^{n-1}(\omega-\Omega)G^1(\Omega). \tag{2.5}$$

This simple convolution equation allows one to compute by recurrence the reduced densities $G^n(\omega)$ starting from the one-phonon density $G^1(\omega)$, which may be measured or estimated easily. The practical importance of Eq. (2.5) is considerable. In fact each recursion step using Eq. (2.3) implies a sampling over a number N of wave vectors in the Brillouin zone. To improve the accuracy of the calculation one needs to increase N and therefore to increase the computational effort required by *each* recursion step. On the contrary, if the recursive convolution of Eq. (2.5) is used, the effort required at each step is independent of N and depends only on the resolution with which $G^n(\omega)$ is desired.

The recursive convolution for $G^n(\omega,\mathbf{k})$ is an easily proved generalization of Eq. (2.5):

$$G^n(\omega,\mathbf{k})=\int d\Omega\ d\mathbf{K}\ G^{n-1}(\omega-\Omega,\mathbf{k}-\mathbf{K})G^1(\Omega,\mathbf{K}). \tag{2.6}$$

We wish to stress that Eqs. (2.3), (2.4), (2.5), and (2.6) do not involve any approximation.

B. Damping from double-vertex diagrams

The simplest double-vertex processes are the ''down'' energy conversion processes. In a ''down'' n-phonon scattering process a phonon 1 with energy ω_1 and wave vector $\mathbf{k}_1$ is annihilated and $n-1$ phonons 2,3,…,n are created. The contribution to the damping Γ_1 of phonon 1 due to ''down'' n-phonon processes ($n\geqslant 3$) is proportional to[5,21]

$$\sum_{\mathbf{k}_2\mathbf{k}_3\cdots\mathbf{k}_n} |V_{1,2,3,\ldots,n}|^2[(n_2+1)(n_3+1)\cdots(n_n+1) -n_2n_3\ldots n_n]\delta[\omega_1-(\omega_2+\omega_3+\cdots+\omega_n)] \times\delta[\mathbf{k}_1-(\mathbf{k}_2+\mathbf{k}_3+\cdots+\mathbf{k}_n)], \tag{2.7}$$

where $V_{1,2,\ldots,n}$ is the nth order anharmonic coupling coefficient and $n_i=[\exp(\hbar\omega_i/k_BT)-1]^{-1}$ is the average phonon occupation number. As shown in the derivation of Eq. (2.7),[5] the factors n_i+1 and n_i originate as thermal averages of ordered products of operators b_i and $b_i^\dagger$, which annihilate and create phonons i:

$$n_i+1=\langle b_ib_i^\dagger\rangle, \qquad n_i=\langle b_i^\dagger b_i\rangle. \tag{2.8}$$

As mentioned in the Introduction, that of Eq. (2.7) is just one of many terms due to all possible combinations of phonon creations and annihilations. The explicit addition of all missing terms would lead to expressions whose complexity increases with n. We avoid this problem by adopting the phonon-antiphonon picture.[5,10] Both positive (phonon) and negative (antiphonon) signs of the phonon energy are allowed and all sums on phonon branches are extended to both energy signs. For a negative energy ω_i (i.e., an antiphonon), the sign of the wave vector $\mathbf{k}_i$ is also inverted and the meaning of the phonon creation and annihilation operators, $b_i^\dagger$ and b_i, are exchanged. Thus the thermal averages n_i+1 and n_i are also exchanged in Eq. (2.7).

Equation (2.7) has the form of a weighted many-phonon density of states, involving $n-1$ phonons. This density may be calculated efficiently using the recurrence relations [Eqs. (2.3) or (2.4)] if the weight may be cast in a factorized form. Each of the two thermal factors in square brackets in Eq. (2.7) is already in the required form. For the coupling coefficients we are forced to adopt a Peierls-type decoupling approximation[5,22] in which $|V_{1,2,\ldots,n}|^2$ is factorized:

$$|V_{1,2,\ldots,n}|^2\propto f(|\omega_1|)f(|\omega_2|)\cdots f(|\omega_n|). \tag{2.9}$$

The function $f(\omega)$ should be chosen to give the correct linear behavior of $|V_{1,2,\ldots,n}|^2$ as one of the phonon frequencies goes to zero.[5,19,23] In the previous paper[5] we chose $f(\omega)=\omega$. Here we prefer $f(\omega)=1-\exp(-\omega/\omega_D)$, where ω_D is the Debye frequency.[19] For small ω, $f(\omega)$ goes linearly to 0 as desired. For $\omega \gg \omega_D$, $f(\omega)$ tends to 1, and thus we avoid the spurious dependence of the coupling coefficients on the phonon frequency which was bothering us in Ref. 5.

Using the approximate factorization of Eq. (2.9), the damping $\Gamma_1^{(n)}$ due to n-phonon double vertex processes, including all combinations of creation and annihilation events, becomes[5]

$$\Gamma_1^{(n)} \propto \sum_{\mathbf{k}_2 \cdots \mathbf{k}_n} [g(\omega_2)g(\omega_3)\cdots g(\omega_n) - g(-\omega_2)g(-\omega_3)\cdots g \times(-\omega_n)]\delta[\omega_1-(\omega_2+\omega_3+\cdots+\omega_n)] \times \delta[\mathbf{k}_1-(\mathbf{k}_2+\mathbf{k}_3+\cdots+\mathbf{k}_n)], \tag{2.10}$$

where all sums extend to both positive and negative energies and we have defined

$$g(\omega)=\begin{cases} f(|\omega|)[n(|\omega|,T)+1] & \text{for } \omega \geqslant 0 \\ f(|\omega|)n(|\omega|,T) & \text{for } \omega \leqslant 0. \end{cases} \tag{2.11}$$

By allowing sums on both signs of the energy, Eq. (2.10) describes any combination of phonon creation and annihilation processes in which a phonon 1 decays with conservation of its energy ω_1 and momentum $\mathbf{k}_1$. In other words, all combinations of phonons and ''antiphonons'' are considered.

The damping $\Gamma_1^{(n)}$ is now expressed as the combination of two densities with factorized weights, each in the form required by Eq. (2.1), and may thus be computed efficiently by using Eqs. (2.4) or (2.6). As the sums in Eq. (2.10) are extended to both energy signs and the Dirac's δ is an even function, it turns out that these two densities represent actually a unique function evaluated at two different places: $G^n(\omega_1,\mathbf{k}_1)$ and $G^n(-\omega_1,-\mathbf{k}_1)$. This is convenient because the recursive algorithm automatically yields the density for all values of ω and $\mathbf{k}$.

For the purposes of this paper, we prefer to neglect the dependence of the densities on the wave vector, replacing them with reduced densities $G^n(\omega)$ [Eq. (2.2)]. This is a very good approximation,[5,13] which enables us to use the simple one-dimensional recursive convolution of Eq. (2.5). We have now discussed all the components of the algorithm for the double vertex damping, which is described in the next section.

III. METHODS

A. Efficient calculation of the many-phonon density of states

As discussed in the Introduction, we advocate a strategy in which the average anharmonic couplings are fitted to the experimental temperature dependence of the damping. The algorithm for computing the damping is based on a representation of the many-phonon density of states as a recursive convolution and involves the following approximations: (1) only the double vertex diagrams are considered, (2) a Peierls type approximation is adopted for the anharmonic coupling coefficients, and (3) the dependence of the density of states on the wave vector is neglected.

We assume that the experimental frequencies ω_i and the linewidth $2\Gamma_i(T)$ as a function of the temperature T are known for a set of phonon branches i. A measured or estimated *unweighted* one-phonon density of states, $D^1(\omega)=\Sigma_{\mathbf{k}i}\delta(\omega-\omega_{\mathbf{k}i})$, is also available, in the form of a numerical histogram in a frequency range $0 \leqslant \omega \leqslant \omega_{\max}$ with some suitable channel width. For definiteness, we normalize $D^1(\omega)$ to a total area equal to the number of phonon branches. With this choice, the numerical value of the density, and thus those of the anharmonic coupling coefficients, does not change if the analysis is restricted to a subset of all phonon branches by neglecting the internal modes or other portions of $D^1(\omega)$.

Starting from $D^1(\omega)$, we evaluate for the range $-\omega_{\max} \leqslant \omega \leqslant \omega_{\max}$ and for a given temperature T the auxiliary temperature dependent density

$$G^1(\omega,T)=\begin{cases} D^1(|\omega|)f(|\omega|)[n(|\omega|,T)+1] & \text{for } \omega \geqslant 0 \\ D^1(|\omega|)f(|\omega|)n(|\omega|,T) & \text{for } \omega \leqslant 0, \end{cases} \tag{3.1}$$

where $n(\omega,T)=[\exp(\hbar\omega/k_BT)-1]^{-1}$ is the average phonon occupation number. For $\omega>0$ or $\omega<0$, this density describes the probability of emission (i.e., creation) or absorption (i.e., annihilation) of a target phonon with frequency $|\omega|$. The thermal weight $n+1$ accounts for both spontaneous and stimulated emission, while n is the weight appropriate to absorption. The factor $f(\omega)=1-\exp(-\omega/\omega_D)$ approximately describes the way in which the anharmonic coupling coefficients go to zero while the phonon frequency goes to zero. The Debye frequency ω_D is simply identified with the largest frequency of the three acoustic branches, and may be found from the density $D^1(\omega)$ as that ω_D for which $\int_0^{\omega_D} d\omega\ D^1(\omega)=3$.

From G^1, we compute a sequence of many-phonon densities G^2, $G^3,\ldots,G^n$, up to the desired order n, using the recursive convolution of Eq. (2.5):

$$G^n(\omega,T)=\int d\Omega\ G^{n-1}(\omega-\Omega,T)G^1(\Omega,T). \tag{3.2}$$

Each G^n is nonzero in the range $-n\omega_{\max} \leqslant \omega \leqslant n\omega_{\max}$, while the integral can be restricted to the range $-\omega_{\max} \leqslant \Omega \leqslant \omega_{\max}$. The structure of Eqs. (3.1) and (3.2) ensures that all G^n's maintain the same physical dimensions as D^1 (the reciprocal of a frequency). The convolution in G^n, being extended to both signs, automatically accounts for all possible combinations of creations and/or annihilations of n target phonons, each one with the proper energy sign and thermal weight. In practice ω is the total energy which the target phonons gain from (for $\omega>0$) or lose to ($\omega<0$) the source phonon. Thus

$$\rho^n(\omega,T)=G^n(\omega,T)-G^n(-\omega,T) \tag{3.3}$$

describes the net (gain-loss) thermally averaged n-phonon population which is available for the decay of a source phonon of frequency ω in a scattering process involving $n+1$ phonons.

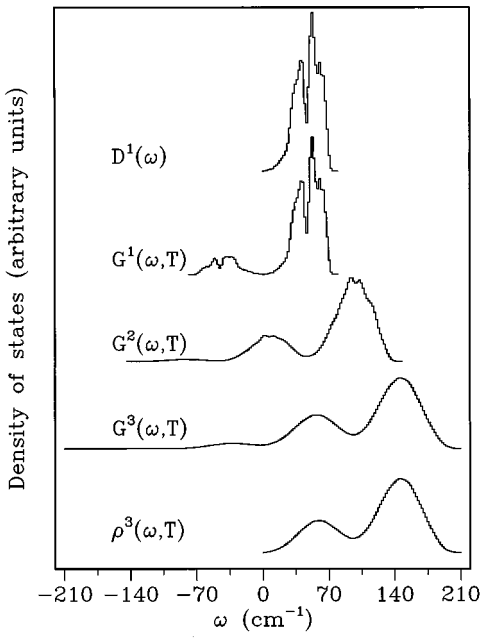

FIG. 1. Calculation of the three-phonon density of states for the lattice modes of α-N_2 at $T=35$ K. From top to bottom: one-phonon density $D^1(\omega)=\Sigma_{\mathbf{k}i}\delta(\omega-\omega_{\mathbf{k}i})$, auxiliary densities $G^1(\omega,T)$ [Eq. (3.1)], $G^2(\omega,T)$ and $G^3(\omega,T)$ [Eq. (3.2)], and thermally weighted density $\rho^3(\omega,T)$ [Eq. (3.3)]. D^1, G^n, and ρ^n are defined for ω in the ranges $[0,\omega_{\max}]$, $[-n\omega_{\max},n\omega_{\max}]$, and $[0,n\omega_{\max}]$, respectively, where $\omega_{\max}\approx 70\ \mathrm{cm}^{-1}$ is the largest lattice frequency.

To illustrate the algorithm for ρ^n just described, we display in Fig. 1 the various steps in the calculation of the three-order density of states for the lattice phonons of N_2 at $T=35$ K. The one-phonon density is first calculated directly from its definition $D^1(\omega)=\Sigma_{\mathbf{k}i}\delta(\omega-\omega_{\mathbf{k}i})$. Details of this calculation appear in Sec. IV. The weighted density $G^1(\omega,T)$ is then obtained from Eq. (3.1). The n-phonon densities $G^2(\omega,T)$ and $G^3(\omega,T)$ are then computed in sequence using the recursive relation (3.2) and finally inserted in Eq. (3.3) to yield the net density $\rho^n(\omega,T)$.

To evaluate the consequences of replacing $G^n(\omega,\mathbf{k})$ with $G^n(\omega)$, we have computed $G^n(\omega,\mathbf{k})$ via Eqs. (2.1) and (2.4). The difference between $G^n(\omega,\mathbf{k})$ and $G^n(\omega)$ is found to be barely noticeable already for $n=2$. Therefore the approximation of neglecting the dependence of the densities on the phonon wave vector is fully justified.

To obtain the total linewidth $2\Gamma_i$ for a phonon at frequency ω_i, we multiply the net n-phonon density ρ^n by the average squared anharmonic coupling coefficient C^i_{n+1} and sum on n:

$$2\Gamma_i(T)=C^i_0+C^i_3\rho^2(\omega_i,T)+C^i_4\rho^3(\omega_i,T)+\cdots+C^i_{n+1}\rho^n(\omega_i,T)+\cdots, \tag{3.4}$$

where a phenomenological parameter C^i_0 has been added to represent any residual temperature independent linewidth not due to many-phonon scattering, such as an instrumental or impurity broadening. The coefficients C^i_n, which depend on the branch index i, may be obtained by fitting Eq. (3.4) to the experimental $\Gamma_i(T)$ or computed from a potential model.[5]

The C^1_n coefficient for a given phonon mode 1 is implicitly defined by comparison of Eq. (3.4) with Eq. (2.7). The corresponding explicit definition[5] in terms of the n-phonon couplings $V_{1,2,3,\ldots,n}$ and of the closely related derivatives $\Phi_{1,2,3,\ldots,n}$ of the total potential with respect to the n normal coordinates associated to $\mathbf{k}_1,\mathbf{k}_2,\mathbf{k}_3,\ldots,\mathbf{k}_n$ (Refs. 9, 19, and 24) is

$$C^1_n=2\pi(n-1)!\,n^2\sum_{\mathbf{k}_2\mathbf{k}_3\cdots\mathbf{k}_n}|V_{1,2,3,\ldots,n}|^2\times[f(\omega_2)f(\omega_3)\cdots f(\omega_n)]^{-1}, \tag{3.5}$$

$$V_{1,2,3,\ldots,n}=\frac{1}{n!}\left(\frac{\hbar}{2\omega_1}\frac{\hbar}{2\omega_2}\frac{\hbar}{2\omega_3}\cdots\frac{\hbar}{2\omega_n}\right)^{1/2}\Phi_{1,2,3,\ldots,n}. \tag{3.6}$$

B. Least squares fit: choice of the model

The fit to the experimental dampings is a typical optimization problem. The damping Γ_e has been measured at a number N of temperatures T_e and a model function $\Gamma(T)$, which depends of a set of undetermined parameters C_n, has been chosen. A combination of parameters which minimizes the distance of the model from the experiment is desired. In situations like the present one, where the experimental errors do not appear to fluctuate wildly and ''outliers'' are not expected, an appropriate measure of distance is the L_2 metric,[25,26] that is the usual χ_2 deviation between measured and model dampings:

$$\chi^2=\sum_{e=1}^{N}\left[\frac{\Gamma_e-\Gamma(T_e)}{\sigma_e}\right]^2. \tag{3.7}$$

The ''weight'' σ_e is the standard deviation of the eth observation. When σ_e is not available, the usual procedure[25,26] is to first assign an arbitrary constant σ to all observations, then fit the model parameters by minimizing χ^2, and finally recompute $\sigma^2=\Sigma_e[\Gamma_e-\Gamma(T_e)]^2/N$. This recipe yields an estimate σ for the standard deviation of the measurements, which will be eventually propagated to an error (i.e., a confidence interval) for the fit parameters.

Because our model equation for $\Gamma(T_e)$, Eq. (3.4), contains, in principle, an infinite number of terms, it is necessary to select an appropriate finite combination of fitting parameters. One has to choose (1) whether to include or not the temperature independent broadening C_0, and (2) the highest order n included in the series. Since low order multiphonon processes are more probable than high order processes, it does not make sense to include a term without including all previous terms in the series.

To provide an example of the problems involved in such a selection, we have chosen two of the phonons of solid N_2, namely the E_g symmetry lattice mode near 38 cm^{-1} and the A_g stretching mode near 2328 cm^{-1}, and separately minimized the χ^2 deviation between the experimental and model damping with several different combinations $\{i,j,\ldots\}$ of nonzero parameters $\{C_i,C_j,\ldots\}$. Figure 2 displays a com-

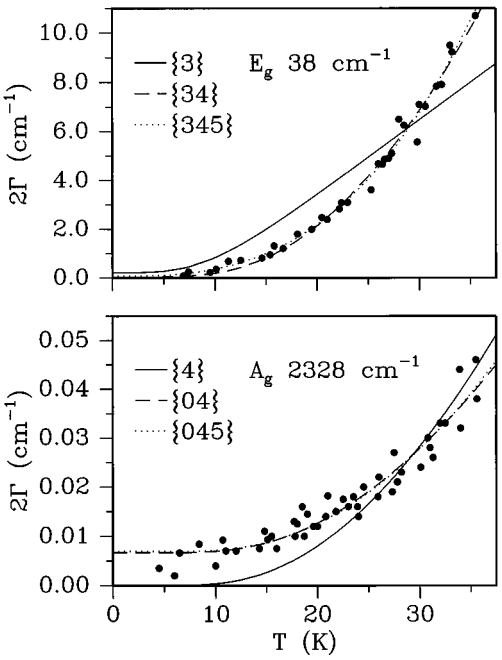

FIG. 2. Choice of the theoretical model for the temperature dependence of the linewidth 2Γ of the E_g lattice mode at 38 cm^{-1} (upper panel) and the A_g stretching mode at 2328 cm^{-1} (lower panel). Circles: experiments (Refs. 14–17); lines: fits with different sets $\{i,j,\ldots\}$ of nonzero coefficients, as indicated in the figure.

parison between the experimental and fitted dampings for some of these combinations. For the phonon at 38 cm^{-1} we also list in Table I the optimal values of the parameters.

For the lattice phonon (upper panel of Fig. 2), the $n=3$ decay processes alone (set {3}) underestimate the observed temperature dependence of the damping, thus indicating that higher order processes are also required. The {34} set performs significantly better, as expected, while the {345} set provides only a very small additional improvement. Since the {03} and {034} sets require negative coefficients (Table I), they are considered as physically meaningless and are not shown in Fig. 2. The constant term C_0 must be excluded from the fit.

For the stretching phonon (lower panel of Fig. 2), there are no $n=3$ decay processes allowed by the energy conservation constraints [i.e., $\rho^2(\omega,T)=0$ for $w=2328$ cm^{-1}]. Because the $n=4$ processes alone (set {4}) overestimate the observed temperature dependence, it is necessary to include C_0, the only possible lower order term. The {04} set reproduces the observations quite well, and, again, the {045} set yields a negligible improvement.

If we were to choose a preferred set of parameters for the lattice mode on an intuitive basis, we would discard the sets {03} and {034} as meaningless, and then adopt the rule of thumb ''keep adding terms until the improvement in the fit becomes small enough'' to select the {34} set as the best and *most informative* set. For the same reason we would select the {04} set for stretching phonon. We aim to formalize and to automate these intuitive notions.

The decision whether to include or not a temperature independent damping C_0 is, in part, a matter of preference. We recall that a source phonon may decay in ''down'' processes in which all of its energy is redistributed by creating a number of phonons of smaller energy, and in various types of ''up'' processes in which the decay is assisted by the additional energy provided by the annihilation of one or more preexisting phonons. At 0 K the thermal phonons population is zero and ''up'' processes are not allowed. Therefore any observed linewidth at very low temperatures must be due to ''down'' decay and/or to the temperature independent broadening C_0.

For the stretching phonons of N_2, due to the structure of the one phonon density of states and to the energy conservation constraints, there are no combinations of phonons available for ''down'' decay. In such cases, which occur frequently for internal phonons, one has to allow for a constant term to reproduce the observed linewidth at 0 K. For N_2 this residual linewidth is $2C_0 \approx 0.005$ cm^{-1} (Fig. 2), a value which is comparable to the statistical error evidenced by the fluctuations of the measurements.

For the lattice phonons the energy conservation constraints for ''down'' decay can always be satisfied. Since both ''down ''decays and temperature independent broadening C_0 contribute to the damping at low temperature, and since for N_2 the latter term appears comparable to the measurement errors, an unambiguous separation of the 0 K linewidth into the two contributions is impossible. In such a situation it is preferable to neglect C_0 with respect to the much larger broadening due to ''down'' decay.

To close this discussion, we summarize our *a priori* recipe for including or not the C_0 term: (1) always include C_0 for those internal phonons for which the structure of the density of states does not allow ''down'' decay; (2) unless there is evidence of structural, isotopical, or chemical disorder, do not include C_0 for all the lattice phonons and for those internal phonons for which ''down'' decay is allowed.

After deciding on the inclusion of the C_0 term, one has to choose the highest order C_n included in the series, a choice which can only be done *a posteriori*. Clearly this choice cannot be based solely on the agreement between measurement and fit. In fact, though the experimental data could be reproduced exactly by using a number of terms (i.e., parameters) equal to the number of measurements, such a fit would contain no useful information beyond that already contained in the data. In some sense, we aim to maximize the additional information provided by the fit.

A reasonable measure of the amount of information in a fit is the Akaike Information Criterion (AIC),[27,28] originally derived in a maximum likelihood context, and defined by

$$\mathrm{AIC}=\ln(\chi^2)+2K, \tag{3.8}$$

where K is the number of adjustable parameters in the model. The model with the minimum AIC is regarded as the best representation of the experimental data. When two different models have almost equal χ^2 deviations, the model with the lower AIC is that with the smaller number of parameters. By minimizing the χ^2 deviation for several alternative models and then by choosing the model with the minimum AIC, one effectively combines a best fit criterion with a ''principle of parsimony.''

We use an AIC analysis to choose the optimal order n for truncating the series for the phonon damping, Eq. (3.4).

TABLE I. Minimum AIC analysis for the E_g mode near 38 cm^{-1}. For each set $\{i,j,\ldots\}$ the table reports the optimal coefficients $C_i, C_j, \ldots$, the AIC and the correlation coefficient $R^2 = \Sigma_e[\Gamma(T_e) - \overline{\Gamma}]^2 / \Sigma_e[\Gamma_e - \overline{\Gamma}]^2$. Here $\Gamma(T)$ is given by Eq. (3.4) and $\overline{\Gamma}$ is the average experimental damping. C_0 is in cm^{-1}; the other coefficients are in cm^{-2}.

Set	AIC	R^2	C_0 cm^{-1}	C_3 cm^{-2}	C_4 cm^{-2}	C_5 cm^{-2}
{3}	5.613	0.876		19.234		
{34}	5.421	0.986		2.845	0.339	
{345}	7.261	0.988		7.678	0.082	0.034
{03}	7.063	0.928	−1.456	24.336		
{034}	7.330	0.987	0.340	−0.350	0.380	

Table I presents the results of such an analysis for the temperature dependence of the damping $\Gamma(T)$ of the phonon at 38 cm^{-1} of N_2. We have separately minimized the χ^2 by including one, two, three, etc. consecutive terms of the series for the damping. For each set $\{i,j,\ldots\}$ the table lists the optimal coefficients $C_i, C_j, \ldots$, together with the corresponding AIC and squared correlation coefficient R^2.

The table clarifies the mechanism through which the AIC analysis weighs accuracy and complexity of the fit function to identify the best model. In the sequence {3}, {34}, {345},..., the AIC first decreases, because the {34} set is much better than the {3} set (R^2 much closer to 1), and then increases, because the very small gain in the fit does not compensate for the cost of additional adjustable parameters. The AIC analysis captures very well our intuitive reasoning and correctly identifies the {34} set as the *most informative* model. Table I also indicates that, as usually expected, the coupling coefficients decrease with increasing order n.

C. Least squares fit: error analysis

The set of parameters $\{C_i^{\min}\}$ which has the minimum AIC and yields the minimum χ^2 distance between measurements and model, $\chi^2_{\min}$, is considered as the ''best'' set. This set of parameters is by no means the ''true'' set, because a repetition of the measurements would yield a different set $\{C_i\}$ of parameters. The probability distribution for $\{C_i\}$, which determines the confidence region for the parameters, obviously depends on the probability distribution for the measurements. If the measurement errors follow a normal (Gaussian) distribution, then it can be proved that the quantity $\Delta\chi^2 = \chi^2(\{C_i\}) - \chi^2_{\min}$ follows a chi-square distribution.[25,26] For each parameter C_i, the regions with $\Delta\chi^2 < 1$, 4, or 9 enclose the 1σ, 2σ, or 3σ interval of confidence (the interval where C_i falls with probability 68.3%, 95.4%, and 99.73%). The recipe mentioned in Sec. III B is to be followed to evaluate σ when the experimental σ_e's are not available.

In the least squares fit for the mode at 38 cm^{-1} we have found that the optimal parameters are not well determined and, as shown by Table I, fluctuate wildly when the number of terms is varied. This pathology is due to the fact that the ''basis functions'' of the problem, i.e., the weighted n-phonon densities of states $\rho^n(\omega,T)$ of Eq. (3.4), are highly correlated to one another. In the limiting case of a perfect correlation, one can build linear combinations of the basis functions exactly equal to zero, and add to the fit arbitrary multiples of such degenerate combinations without any effect on the χ^2. Even this singular situation does not imply that the fit is totally meaningless, but merely that the coefficient in front of a degenerate combination is undetermined. The coefficients of other combinations may well be determined with high precision.

The recommended method for singular, or close to singular, χ^2 problems is singular value decomposition (SVD). As the SVD algorithm is described in many numerical analysis handbooks,[25,26] we will simply summarize the main principles of the method. Because the theoretical dampings $\Gamma(T)$ of Eq. (3.4) are linear in the fit parameters $\{C_i\}$, the χ^2 deviation of Eq. (3.7) is a second order polynomial in $\{C_i\}$. The surface $\Delta\chi^2 = \text{const}$ is therefore a quadratic form, which describes a multidimensional ellipsoid centered on $\{C_i^{\min}\}$. The SVD procedure is mathematically analogous to the diagonalization of a dynamical matrix which gives the eigenvectors and eigenfrequencies of a set of coupled harmonic oscillators; SVD yields an orthonormal set of vectors $\mathbf{V}_j$ describing the principal axes of the ellipsoid in terms of the original parameters, and a corresponding set of ''singular values'' w_j whose reciprocals are the axis lengths. The procedure returns in effect a rotation from the old parameters $\{C_i - C_i^{\min}\}$ to a new set of parameters $\{A_j\}$ which diagonalize the $\Delta\chi^2$ quadratic form:

$$\Delta\chi^2 = w_1^2 A_1^2 + w_2^2 A_2^2 + \cdots + w_n^2 A_n^2. \tag{3.9}$$

The absence of cross terms in Eq. (3.9) indicates that the new parameters A_j are mutually independent (statistically uncorrelated). Those combinations $\mathbf{V}_j$ of the original parameters with the larger w_j have the larger effect on the fit and are therefore the more precisely determined combinations.

IV. CALCULATIONS

We present here the details of the test calculation for α-N_2. Solid nitrogen in its α phase crystallizes as a cubic lattice (space group $Pa3$, T_h^6) and is stable in the temperature range 0–36 K.[29] The factor group analysis of the $\mathbf{k}=0$ lattice modes predicts five Raman active modes (with symmetry $A_g + E_g + 3T_g$), two infrared active modes ($2T_u$), two optically inactive modes ($A_u + E_u$), and one acoustic mode (T_u). The experimental temperature dependence of the damping, $\Gamma(T)$, is available for most of the active modes.[14–18] For each of these modes i we have estimated the average anharmonic coupling coefficients C_n and their confidence regions by fitting the experimental $\Gamma_i(T)$.

The one-phonon density, $D^1(\omega) = \Sigma_{\mathbf{k}i}\delta(\omega - \omega_{\mathbf{k}i})$, has been calculated by sampling the full Brillouin zone (BZ) with about 10 000 wave vectors. The phonon frequencies have been computed at the extrapolated 0 K crystal structure[30] with the intermolecular potential model of Murthy *et al.*,[31] to which we have added a purely harmonic intramolecular potential.[5] The Debye frequency, estimated by integrating $D^1(\omega)$, is $\omega_D = 33.3$ cm^{-1}. The recursive algorithm described in Sec. III A has then been used to compute the thermally weighted n-phonon densities [Eq. (3.3)] $\rho^n(\omega,T)$ up to $n=5$, for all temperatures T at which Γ has been measured. These densities, evaluated at the mode fre-

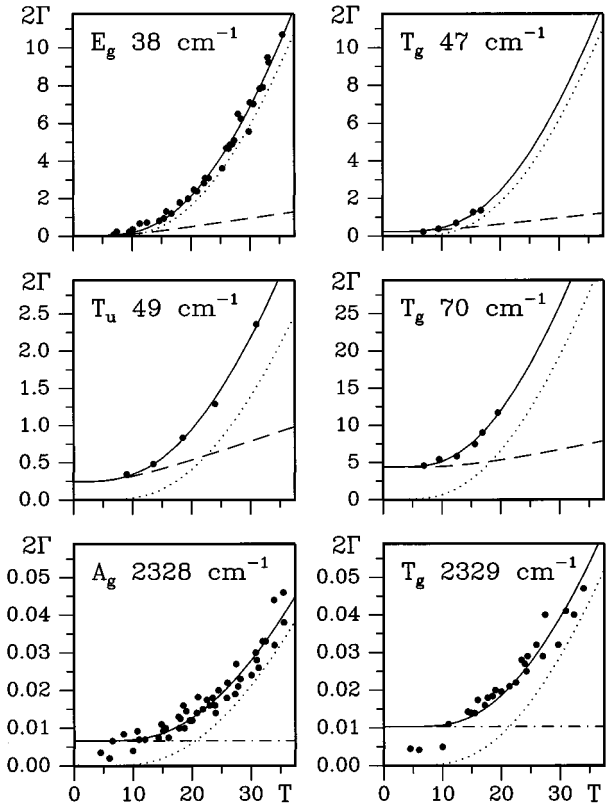

FIG. 3. Linewidth 2Γ (cm^{-1}) vs temperature T (K) for the phonons of α-nitrogen. Phonon modes are labeled by their symmetry species and calculated harmonic frequency in cm^{-1}. Circles denote experiments (Refs. 14–18). Linestyles distinguish fit results: total linewidth (solid lines); individual contributions due to C_0 (dash-dot), C_3 (dashes), and C_4 (dots).

quency ω_i, are to be inserted in the model equation for the fit [Eq. (3.4)].

Minimum AIC fits have been performed for all phonon modes i for which experimental $\Gamma_i(T)$'s are available. All sets of consecutive nonzero coefficients, C_3, C_4, C_5, and C_6, have been tested. As previously discussed, the constant term C_0 has been included only for the stretching modes. To provide a worked example of the connection between potential model and C_n coefficients, we have also computed C_n through Eqs. (3.5) and (3.6). The potential derivatives have been computed numerically, as described in Ref. 5.

V. RESULTS

The results of the fits are shown in Fig. 3. We have found that the {34} set has the best AIC for all lattice modes, whereas the {04} set has the best AIC for the two stretching phonons. As shown in Fig. 3, the dominant contribution to the width at higher temperatures is given in all cases by the diagrams of vertex order $n=4$. This conclusion is in agreement with the *a priori* calculations.[5] The anharmonic coupling coefficients C_n obtained from the fits are listed in Table II together with the *a priori* C_n calculated from the potential. The calculated coefficients of Table II are different from those of Ref. 5, due to a different choice for the weight function, to changes of units, and to a programming error for the stretching modes.

Both fitted and calculated C_n decrease quite fast with increasing order n. In this respect the *a priori* computation confirms the results of the AIC analysis, and indicates that for α-N_2 the n-phonon processes beyond $n=4$ are not very important with respect to three- and four-phonon processes.

A more meaningful comparison between *a priori* computation and fit depends on the confidence region of the fit. The SVD confidence ellipsoids for the fit coefficients are shown in Fig. 4 together with the *a priori* coefficients. Each ellipsoid $\Delta\chi^2 \leqslant 9$, whose principal axes have orientation $\mathbf{V}_j$ and length $1/w_j$, encloses the 3σ confidence region for the coefficients C_3 and C_4 (or C_0 and C_4) for a single mode. For all lattice modes, the ellipsoids are very elongated and have a negative slope for the major axis, thus indicating a negative correlation between C_3 and C_4. Thus substantial variations of C_3, compensated by smaller variations of C_4 in the opposite direction, are allowed by the fit data. Previous

TABLE II. Anharmonic coupling coefficients C_i obtained from the AIC fit to the experimental linewidths and calculated as averages of potential derivatives according to Eqs. (3.5) and (3.6). Phonon modes are labeled by their symmetry species and calculated harmonic frequency.

Sym.	Freq. cm^{-1}		C_0 cm^{-1}	C_3 cm^{-2}	C_4 cm^{-2}	C_5 cm^{-2}
E_g	38	Fit		2.845	0.339	
		Calc.		2.158	0.202	2.913×10^{-3}
T_u	45	Fit		2.749	0.055	
		Calc.		2.343	0.226	4.762×10^{-3}
T_g	47	Fit		3.632	0.261	
		Calc.		3.387	0.219	3.601×10^{-3}
T_g	70	Fit		3.294	0.754	
		Calc.		2.647	0.115	2.557×10^{-3}
A_g	2328	Fit	0.666×10^{-2}		0.129×10^{-2}	
		Calc.		0.075	2.200×10^{-5}	2.756×10^{-8}
T_g	2329	Fit	0.103×10^{-1}		0.167×10^{-2}	
		Calc.		0.101	6.608×10^{-5}	3.132×10^{-8}

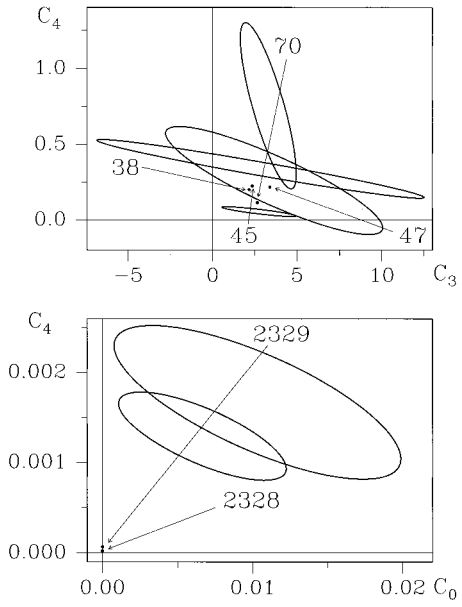

FIG. 4. Anharmonic coupling coefficients C_n for the lattice and the stretching modes (upper and lower panel, respectively). C_3 and C_4 are in cm^{-2} units; C_0 in cm^{-1}. Symbols: coefficients computed as averages of potential derivatives. Ellipsoids: 3σ parameter confidence region obtained from the SVD analysis. Harmonic frequencies (cm^{-1}) label nearby ellipsoids and, as indicated by the arrows, corresponding calculated coefficients.

studies[9,12,32] indicate that large ambiguities in the fit parameters are a common occurrence. As shown by Fig. 4, the *a priori* C_n are not particularly well correlated to the fitted C_n, although they usually lie within or close to the 3σ confidence region of the fit. Please note that the regions corresponding to negative coefficients, though allowed by the fit, must be rejected on physical grounds.

The C_0 and C_4 coefficients for the stretching modes are both well determined ($\sigma \approx 10\%$) and exhibit a rather weak cross correlation (the axes of the ellipsoids do not deviate much from the C_0 and C_4 axes). For these modes the comparison between fit and calculation is quite problematic, since C_3 is not experimentally accessible, due to the absence of two-phonon resonances around $2328-2329\ cm^{-1}$, and C_0 has a purely phenomenological origin without a well defined *a priori* equivalent. For C_4, the only coefficient for which a comparison is possible, the results obtained from the potential derivatives are substantially smaller than those obtained from the fit.

Our results cannot be directly compared to the anharmonic constants obtained from a phenomenological fit for the T_u mode,[18] since this includes the state density factor also. Comparison of the temperature dependence of the cubic and quartic contributions to the linewidth in the two cases indicates, however, that the two methods lead to essentially the same results.

VI. DISCUSSION AND CONCLUSIONS

We have developed a very efficient method to calculate the phonon damping in anharmonic crystals starting from the one-phonon density of states and the average anharmonic couplings between phonons. The one-phonon density is used to obtain the n-phonon thermally weighted densities which, when multiplied by the coupling coefficients, yield the various high order contributions to the phonon damping. For α-N_2 we have obtained the coupling coefficients C_n in two different ways: by averaging potential derivatives, with the potential model of Murthy *et al.*,[31] and by fitting the experimental temperature dependence of the phonon damping. Criteria for choosing an optimal combination of decay processes and methods to estimate the confidence region of the coefficients have been presented in the context of the fit.

For the lattice modes of α-N_2 the calculated coefficients C_3 and C_4 are of the same magnitude as those obtained from the fit, although considerable deviations exist among the different modes. For the stretching modes, the calculated C_4 coefficients are much smaller than those from the fit. This situation corresponds to that found in most past calculations for the damping,[12,33–36] which were usually restricted to $n=3$ processes. The $n=3$ results for the lattice modes of N_2 (Refs. 33 and 34) indicate that different potential models with comparable harmonic frequencies may give surprisingly large linewidth differences. Furthermore, it should be noted that in calculations like the present one[5,12,37] the *a priori* average coupling C_4 has been estimated by sampling over a restricted class of coefficients. Therefore, C_4 is expected to be less accurate than C_3, which is averaged over all coefficients. This expectation is consistent with the results of the fit. For the lattice modes, the *a priori* C_3 lie within the confidence region of the fit, whereas this does not apply for C_4.

In the calculations for the $n=3$ contribution to the decay of internal modes[12,35,38] (for systems where $n=3$ decays are allowed) the experimental linewidth was also systematically underestimated. These findings indicate that detailed agreement between the fitted and computed C_n can only be obtained by fine tuning of the potential model. Intramolecular anharmonicity, totally neglected in the present calculations, is probably to be blamed for most of the discrepancies found for the stretching modes.

The methods discussed in this paper provide a systematic strategy for extracting information on the potential anharmonicity from the experimental temperature dependence of the phonon linewidths and a rational way of comparing the extracted information with a potential model.

ACKNOWLEDGMENTS

This work was supported by Italian CNR and MURST. We thank Carlo Camaggi and Piero Salvi for valuable suggestions.

*Author to whom correspondence should be addressed.

[1] A. A. Abrikosov, L. P. Gorkov, and I. E. Dzyaloshinski, *Methods of Quantum Field Theory in Statistical Mechanics* (Prentice-Hall, Englewood Cliffs, NJ, 1963).

[2] A. L. Fetter and J. B. Walecka, *Quantum Theory of Many Particle Systems* (McGraw-Hill, New York, 1971).

[3] A. A. Maradudin and A. Fein, Phys. Rev. **128**, 2589 (1962).

[4] R. S. Tripathy and K. N. Pathak, Nuovo Cimento **21**, 286 (1974).

[5] P. Procacci, G. F. Signorini, and R. G. Della Valle, Phys. Rev. B **47**, 11 124 (1993). Please notice that $G_{+}^{(n+1)}$ of this reference corresponds to G^{n} of the present work and that in this reference we had not yet realized that $G_{-}^{(n)}(\omega,\mathbf{k})=G_{+}^{(n)}(-\omega,-\mathbf{k})$.
[6] M. R. Monga and K. N. Pathak, Phys. Rev. B **18**, 5859 (1978).
[7] V. K. Jindal, R. Righini, and S. Califano, Phys. Rev. B **38**, 4259 (1989).
[8] P. Procacci, G. Cardini, R. Righini, and S. Califano, Phys. Rev. B **45**, 2113 (1992).
[9] S. Califano and V. Schettino, Int. Rev. Phys. Chem. **7**, 19 (1988) and references therein.
[10] R. G. Della Valle and P. Procacci, Phys. Rev. B **46**, 6141 (1992).
[11] T. Sato and T. Asari, J. Phys. Soc. Jpn. **64**, 1193 (1995).
[12] G. F. Signorini, M. Becucci, and E. Castellucci, Chem. Phys. **187**, 263 (1994).
[13] R. G. Della Valle and G. Cardini, Phys. Rev. Lett. **59**, 2196 (1987).
[14] R. Ouillon, C. Turc, J. P. Lemaistre, and P. Ranson, J. Chem. Phys. **93**, 3005 (1990).
[15] R. D. Beck, M. F. Hineman, and J. W. Nibler, J. Chem. Phys. **92**, 7068 (1990).
[16] J. De Kinder, E. Goovaerts, A. Bouwen, and D. Schoemaker, Phys. Rev. B **42**, 5953 (1990).
[17] J. De Kinder, E. Goovaerts, A. Bouwen, and D. Schoemaker, J. Lumin. **53**, 72 (1992).
[18] R. Bini, J. Chem. Phys. **104**, 4365 (1996).
[19] M. Born and K. Huang, *Dynamical Theory of Crystal Lattices* (Oxford University Press, New York, 1954).
[20] H. S. Wilf, *Algorithms and Complexity* (Prentice-Hall, Englewood Cliffs, NJ, 1986).
[21] A. Nitzan, S. Mukamel, and J. Jortner, J. Chem. Phys. **60**, 3929 (1973).
[22] R. E. Peierls, *Quantum Theory of Solids* (Oxford University Press, New York, 1955).
[23] R. G. Della Valle, P. F. Fracassi, V. Schettino, and S. Califano, Chem. Phys. **43**, 385 (1979).
[24] R. G. Della Valle, P. F. Fracassi, R. Righini, and S. Califano, Chem. Phys. **74**, 179 (1983).
[25] W. Menke, *Geophysical Data Analysis: Discrete Inverse Theory* (Academic, Orlando, FL, 1984).
[26] W. H. Press, B. P. Flannery, S. A. Teukolsky, and W. T. Vetterling, *Numerical Recipes* (Cambridge University Press, Cambridge, England, 1986).
[27] H. Akaike, IEEE Trans. Automat. Contr. **AC-19**, 716 (1974).
[28] K. Yamaoka, T. Nakagawa, and T. Uno, J. Pharmacokin. Biopharm. **6**, 165 (1978).
[29] J. K. Kjems and G. Dolling, Phys. Rev. B **11**, 1639 (1975).
[30] I. N. Krupskii, A. I. Prokhvatilov, and A. I. Erenburg, Sov. J. Low Temp. Phys. **1**, 178 (1975).
[31] C. S. Murthy, S. F. O'Shea, and I. R. McDonald, Mol. Phys. **50**, 531 (1983).
[32] C. Taiti, P. Foggi, G. F. Signorini, and V. Schettino, Chem. Phys. Lett. **212**, 283 (1993).
[33] K. Kobashi and V. Chandrasekharan, Mol. Phys. **36**, 1645 (1978).
[34] G. F. Signorini, P. F. Fracassi, R. Righini, and R. G. Della Valle, Chem. Phys. **100**, 315 (1985).
[35] R. G. Della Valle and R. Righini, Chem. Phys. Lett. **148**, 45 (1988).
[36] P. Foggi and V. Schettino, Nuovo Cimento **15**, 1 (1992).
[37] G. F. Signorini, C. Taiti, and B. Caldarone, Mol. Cryst. Liq. Cryst. (to be published).
[38] G. F. Signorini, Ph.D. thesis, Università di Firenze, Firenze, Italy, 1989.